

# Diffusion-weighted MR Imaging of the Normal Human Spinal Cord in Vivo

Chad A. Holder, Raja Muthupillai, Srinivasan Mukundan, Jr, James D. Eastwood, and Patricia A. Hudgins

**BACKGROUND AND PURPOSE:** Diffusion-weighted imaging is a robust technique for evaluation of a variety of neurologic diseases affecting the brain, and might also have applications in the spinal cord. The purpose of this study was to determine the feasibility of obtaining in vivo diffusion-weighted images of the human spinal cord, to calculate normal apparent diffusion coefficient (ADC) values, and to assess cord anisotropy.

**METHODS:** Fifteen healthy volunteers were imaged using a multi-shot, navigator-corrected, spin-echo, echo-planar pulse sequence. Axial images of the cervical spinal cord were obtained with diffusion gradients applied along three orthogonal axes (6 b values each), and ADC values were calculated for white and gray matter.

**RESULTS:** With the diffusion gradients perpendicular to the orientation of the white matter tracts, spinal cord white matter was hyperintense to central gray matter at all b values. This was also the case at low b values with the diffusion gradients parallel to the white matter tracts; however, at higher b values, the relative signal intensity of gray and white matter reversed. With the diffusion gradients perpendicular to spinal cord, mean ADC values ranged from 0.40 to  $0.57 \times 10^{-3}$  mm<sup>2</sup>/s for white and gray matter. With the diffusion gradients parallel to the white matter tracts, calculated ADC values were significantly higher. There was a statistically significant difference between the ADCs of white versus gray matter with all three gradient directions. Strong diffusional anisotropy was observed in spinal cord white matter.

**CONCLUSION:** Small field-of-view diffusion-weighted images of the human spinal cord can be acquired in vivo with reasonable scan times. Diffusion within spinal cord white matter is highly anisotropic.

MR diffusion-weighted imaging has proven to be a robust technique for the evaluation of a variety of neurologic diseases, both as a research tool and in clinical practice, although its use has been largely limited to the brain (1–14). Early on, it was recognized that water mobility within the brain was not uniform in all directions, a phenomenon known as diffusional anisotropy, and that this could affect the signal intensity of normal tissues on diffusion-weighted images and, therefore, the interpretation of the images. Diffusional anisotropy within cere-

bral white matter tracts has been demonstrated qualitatively and measured quantitatively, and calculated apparent diffusion coefficient (ADC) values for normal human cerebral gray and white matter have been published (8, 9, 15, 16).

As with diffusion imaging of the brain, knowledge and understanding of the appearance of the normal spinal cord on diffusion-weighted images will be important for the interpretation of images of the abnormal cord in a clinical setting. An understanding of the diffusion characteristics of the normal spinal cord will also be useful in designing pulse sequences and imaging protocols to identify areas of abnormal diffusion optimally. Unlike diffusion imaging of the brain, however, experience with diffusion imaging of the spinal cord is much more limited. In 1991, Hajnal et al (9) noted anisotropic diffusion qualitatively in normal human spinal cord. Since that time, however, there have been few published reports of in vivo diffusion imaging of the human spinal cord (17). We sought to implement and optimize an echo planar–based diffusion-weighted MR pulse sequence that would allow in vivo spinal cord imaging with practical scan

---

Received November 18, 1998; accepted after revision May 4, 2000.

From the Department of Radiology (C.A.H., S.M., J.D.E., P.A.H.), Emory University School of Medicine, Atlanta, GA and Philips Medical Systems North America (R.M.), Shelton CT.

Presented at the annual meeting of the American Society of Neuroradiology, Philadelphia, May 1998.

Address reprint requests to Chad A. Holder, MD, Assistant Professor of Radiology, Emory University School of Medicine, Department of Radiology, Emory University Hospital/B115, 1364 Clifton Rd, NE, Atlanta, GA 30322.

© American Society of Neuroradiology

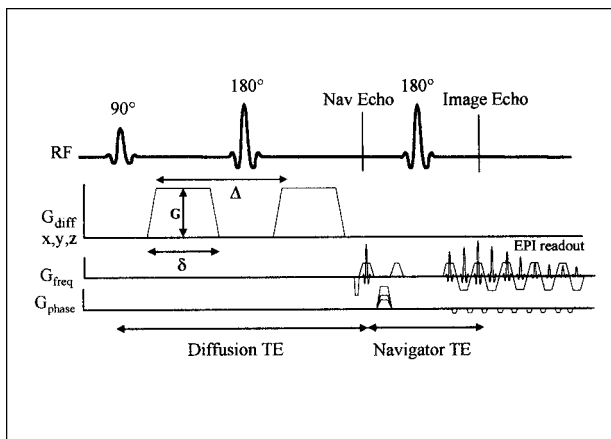


FIG 1. Navigator-corrected, multi-shot, spin-echo echo-planar pulse sequence with diffusion-sensitizing gradients of amplitude ( $G$ ), duration ( $\delta$ ), and separation ( $\Delta$ ). The diffusion gradients can be applied along any imaging direction. The navigator echo (the first spin-echo of this dual echo sequence) is not spatially encoded, and is used for phase correction of the second echo.

times. Additional goals were to determine the appearance of the normal human spinal cord on diffusion-weighted images, to measure normal ADC values, and to assess for diffusional anisotropy.

## Methods

### Study Population

The study population consisted of 15 neurologically healthy volunteers (age range, 23–34 years; 12 men, 3 women) who were recruited within the guidelines of our Institutional Review Board and Human Investigations Committee. All subjects underwent screening MR imaging of the cervical spine, consisting of sagittal T1-weighted spin-echo (500/18/2 [TR/TE/excitations]) and T2-weighted turbo spin-echo (2800/120/1) images. Screening MR imaging was performed on the same day as diffusion imaging in order to exclude unsuspected signal abnormality within the spinal cord.

### Image Acquisition

All imaging was performed on a commercial 1.5-T MR scanner (ACS-NT; Philips Medical Systems; Best, The Netherlands) equipped with echo-planar gradients (23-mT/m maximum gradient strength, 200- $\mu$ s rise time) and standard phased-array spine surface coil as the receiver coil. Diffusion-weighted imaging was performed using a multi-shot, spin-echo echo-planar pulse sequence with the following parameters: TR = 2  $\times$  R-R interval (approximately 2000 ms, depending on heart rate); total TE = 106 ms (diffusion TE = 85 ms, navigator TE = 21 ms); excitations = 4; field of view = 10  $\times$  10 cm; acquisition matrix = 64  $\times$  64 (reconstructed 128  $\times$  128); echo-planar imaging factor = 15; slice thickness = 6 mm. Peripheral pulse unit (PPU) triggering, navigator-echo motion correction (18–22), and segmented signal averaging (serial motion artifact reduction technique [SMART]) were used to minimize the effects of motion. Fat suppression and fold-over suppression were also used. The acquisition time ranged from 184 to 216 s per diffusion direction, depending upon heart rate. The simplified pulse sequence diagram is shown in Figure 1.

Axial diffusion-weighted images of the cervical spinal cord were obtained at seven slice levels, centered at the C4-C5 intervertebral disk space. Diffusion-sensitizing gradients were applied along each of three orthogonal axes by use of six “b” values (0, 40, 160, 360, 640, 1000 s/mm<sup>2</sup>). The PPU triggering

TABLE 1: ADC values of white versus gray matter in the axial imaging plane

	R-L ( $\times 10^{-3}$ mm <sup>2</sup> /s)	A-P ( $\times 10^{-3}$ mm <sup>2</sup> /s)	C-C ( $\times 10^{-3}$ mm <sup>2</sup> /s)
WM	0.44 $\pm$ 0.19	0.40 $\pm$ 0.32	2.26 $\pm$ 0.88
GM	0.55 $\pm$ 0.18	0.57 $\pm$ 0.33	1.98 $\pm$ 0.86

enabled the acquisition of data for a given slice at the same cardiac phase over the duration of the scan. Hence, different slices were obtained at different trigger delays. Specific trigger delays were as follows: slices 1 and 2 at 117 ms; slices 3 and 4 at 338 ms; slices 5 and 6 at 559 ms; and slice 7 at 781 ms.

Initial validation of the diffusion-weighted sequence was performed by measuring the ADC values of a 1-L water/copper sulfate phantom at ambient temperature (approximately 22°C).

### Image Analysis

ADC values were calculated from signal intensity measurements obtained from the axial diffusion-weighted images by use of four regions of interest (ROIs) placed in the right lateral white matter, left lateral white matter, right gray matter, and left gray matter, in a manner similar to that described by Patany et al (23). For each volunteer, ROIs were carefully drawn on two of the seven slices on the MR console by an experienced neuroradiologist (CAH). The third and fifth slices were used for the ROI measurements, unless one of the slices was deemed unacceptable for ROI measurements due to gross motion artifact, in which case an alternative slice was chosen (either the second, fourth, or sixth slice), so as to exclude spurious data corrupted by noise. This resulted in a total of 2160 individual ROI measurements (15 volunteers, two slices/volunteer, six b values, three directions/slice, and four ROIs/image). It was not possible to perform ROI measurements on all slices owing to the sheer number of measurements that would have been required. When performing the ROI measurements, small ROIs were intentionally drawn in an attempt to reduce the likelihood of partial volume averaging between gray and white matter and between white matter and CSF. The size of the axial ROIs ranged from nine to 11 pixels. The placement of the ROIs was based upon both the b = 0 (T2-weighted echo-planar) images and the diffusion-weighted images, as well as the knowledge of the cross-sectional anatomy of the normal human cervical spinal cord.

ADC values were calculated from the ROI signal intensity measurements, based upon the relationship:  $S = S_0 e^{-bD}$ , where  $D = \text{ADC}$ . In order to obtain more accurate ADC measurements, the ADC values were calculated by using six different b values. A least squares curve fitting algorithm was used to calculate the ADCs from the exponential signal intensity decay curve.

### Statistics

The statistical significance of the computed mean ADC values of gray versus white matter was assessed using a paired, double-tailed Student's *t* test ( $P < .05$  was considered statistically significant).

## Results

Using the mean ADC values for the three diffusion directions, anisotropy indices were calculated for spinal cord white matter and gray matter, respectively, as described by Douek et al (24). The anisotropy index is a ratio that reflects the magnitude of the difference between ADC values in one

direction compared with another. A tissue or substance with isotropic diffusion, such as free water, will have an anisotropy index of 1.0. Comparing the measured ADC values with the diffusion-sensitizing gradients in the C-C direction to the average of the ADCs with the diffusion gradients in the axial plane (A-P and R-L), the anisotropy index of spinal cord white matter was found to be 5.38, and the anisotropy index of central gray matter was 3.53.

### Discussion

MR diffusion-weighted imaging has been used to study a variety of diseases affecting the central nervous system, both as a research tool and in clinical practice, and has been widely adopted for the evaluation of cerebral ischemia. In the brain, water mobility of altered tissue, reflecting underlying structural changes on a microscopic level, has been demonstrated in cerebral infarction (1–3), multiple sclerosis (4–5), traumatic brain injury (6), neoplasms (7–9), abscesses (10), encephalitis (11), and reversible posterior leukoencephalopathy syndromes, such as eclampsia (12), hypertensive encephalopathy (13), and immunosuppressant neurotoxicity (14).

Diffusion imaging might also be useful for evaluating analogous conditions in the spinal cord. Clinical and research experience with diffusion-weighted imaging of the spinal cord, however, is much more limited. This is primarily because of technical difficulties in obtaining *in vivo* diffusion images in this location. Much of the accrued experience to date has been in animal spinal cords, both excised and *in vivo*, using dedicated small-bore animal magnets and/or customized receiver coils. The diffusion imaging appearance and ADC values have been reported for excised normal animal spinal cords (23, 25–27), in a spinal cord injury model (28), and in a rat model of syringomyelia (29). *In vivo* diffusion anisotropy has also been described qualitatively in cats (30) and rats (31, 32). In 1991, Hajnal and coworkers (9) published the first *in vivo* DW images of the human cervical spinal cord. Other investigators have reported their preliminary experience using a steady-state free precession technique (33, 34), although, to our knowledge, these results have not yet been published. More recently, a navigated pulsed-gradient spin-echo method was used to study four volunteers, in which images of the cervical spinal cord were obtained with diffusion sensitization in the anteroposterior and superoinferior directions, as well as ADC maps (17). Unfortunately, the imaging time of approximately 30 minutes (15 minutes per diffusion-sensitization direction) to obtain four sagittal slices, as well as the off-line processing required to correct for motion artifacts, makes this technique impractical for routine clinical use.

The main technical obstacles in obtaining diffusion-weighted images of the human spinal cord *in vivo*

are twofold: the small size of the spinal cord and physiological motion. The navigator-guided, multi-shot echo-planar technique made it possible to obtain submillimeter (effective) in-plane resolution diffusion images of the human spinal cord *in vivo* in this study. When compared with single-shot techniques (that typically use echo-planar factors of 63 or greater), the shorter readout duration in the multi-shot technique permits a shorter TE. This improves signal-to-noise ratio (SNR) and is less sensitive to off-resonance effects, such as those caused by field inhomogeneity and chemical shift, resulting in improved image quality (35). The trade-off for using a multi-shot echo-planar technique is that the acquisition time increases, making this technique vulnerable to patient motion. In the present study, to offset this concern, a navigator echo-based phase-correction method was implemented. This correction addresses the effect of linear motion that may occur between excitations (18–22). In addition, the main advantage of the navigator-based multi-shot technique for diffusion imaging is that it makes it possible to extend the duration of the acquisition. This flexibility permits the acquisition of images with higher spatial resolution (smaller voxels) by making it possible to obtain multiple signal averages (excitations) to improve SNR and compensate for the decreased SNR associated with smaller voxels, as was done in this study. PPU triggering was used to trigger the acquisitions to minimize the effects of cardiac-synchronous motion in both CSF flow and the spinal cord, which is particularly problematic in spinal imaging.

Anatomic coverage is another clinically relevant issue. Although axial slices were useful to compute the ADC values, the time required to cover the entire cervical spinal cord with axial slices at this resolution would be prohibitively high. Therefore, we have also obtained sagittal sections to ensure adequate coverage in the shortest possible time. Our initial experimental results are shown in Figure 3. Our preliminary experiments ( $n = 5$ ) show that the ADC values computed with sagittal orientation were consistent with ADC measurements obtained from the axial orientation. However, it was not possible to distinguish gray and white matter in this orientation.

The results of this study confirm the presence of strong diffusional anisotropy in human spinal cord white matter. The longitudinal ADC values that were obtained for cord white matter are higher than published values for cerebral white matter. This is likely because, in the brain, unlike the spinal cord, any ROI is more likely to contain varying numbers of axons at oblique orientations with respect to the applied diffusion gradients. This would result in a lower measured ADC for a given diffusion direction.

The longitudinal ADC values we obtained in human spinal cord white matter are also higher than some previously published values for animal spinal

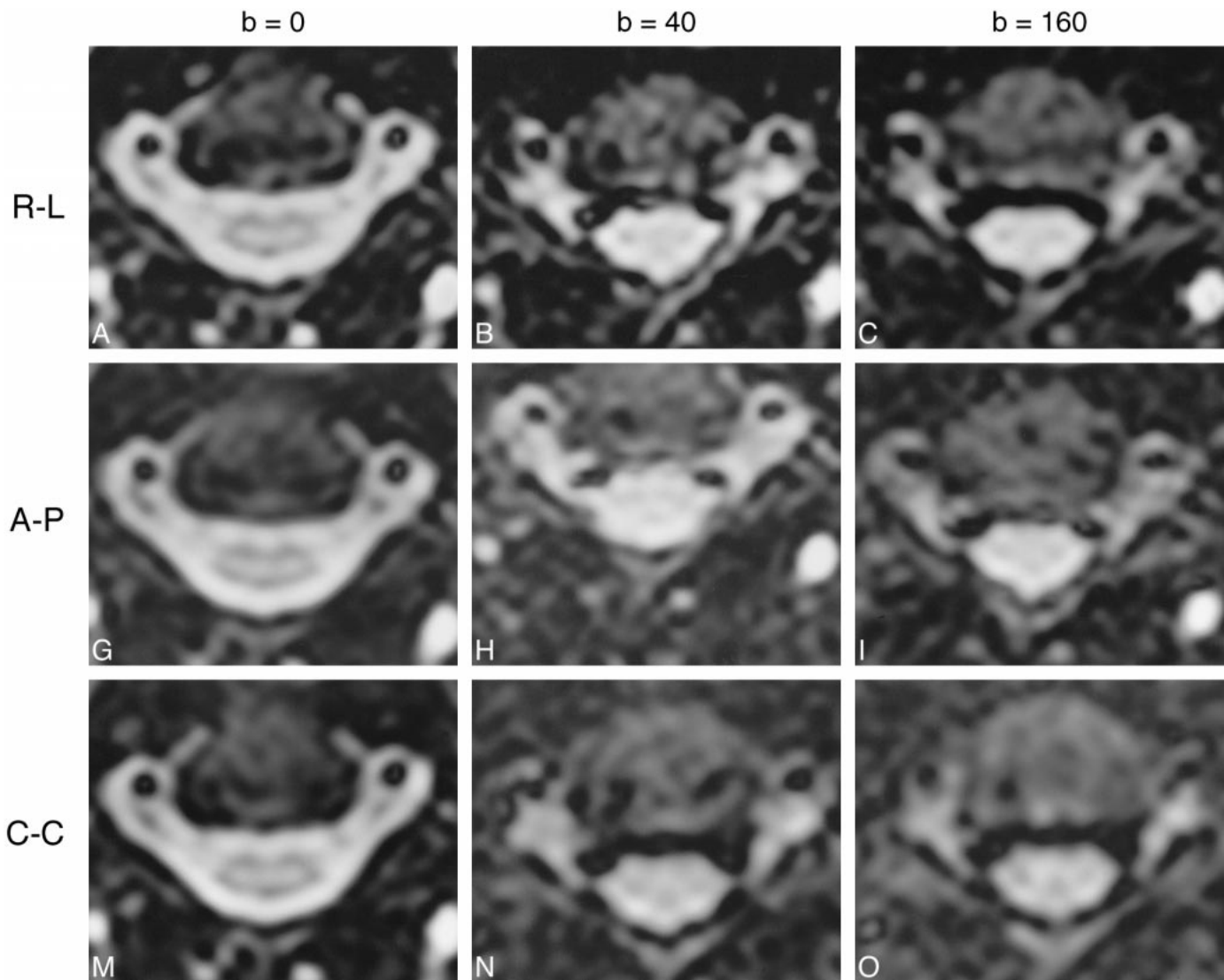
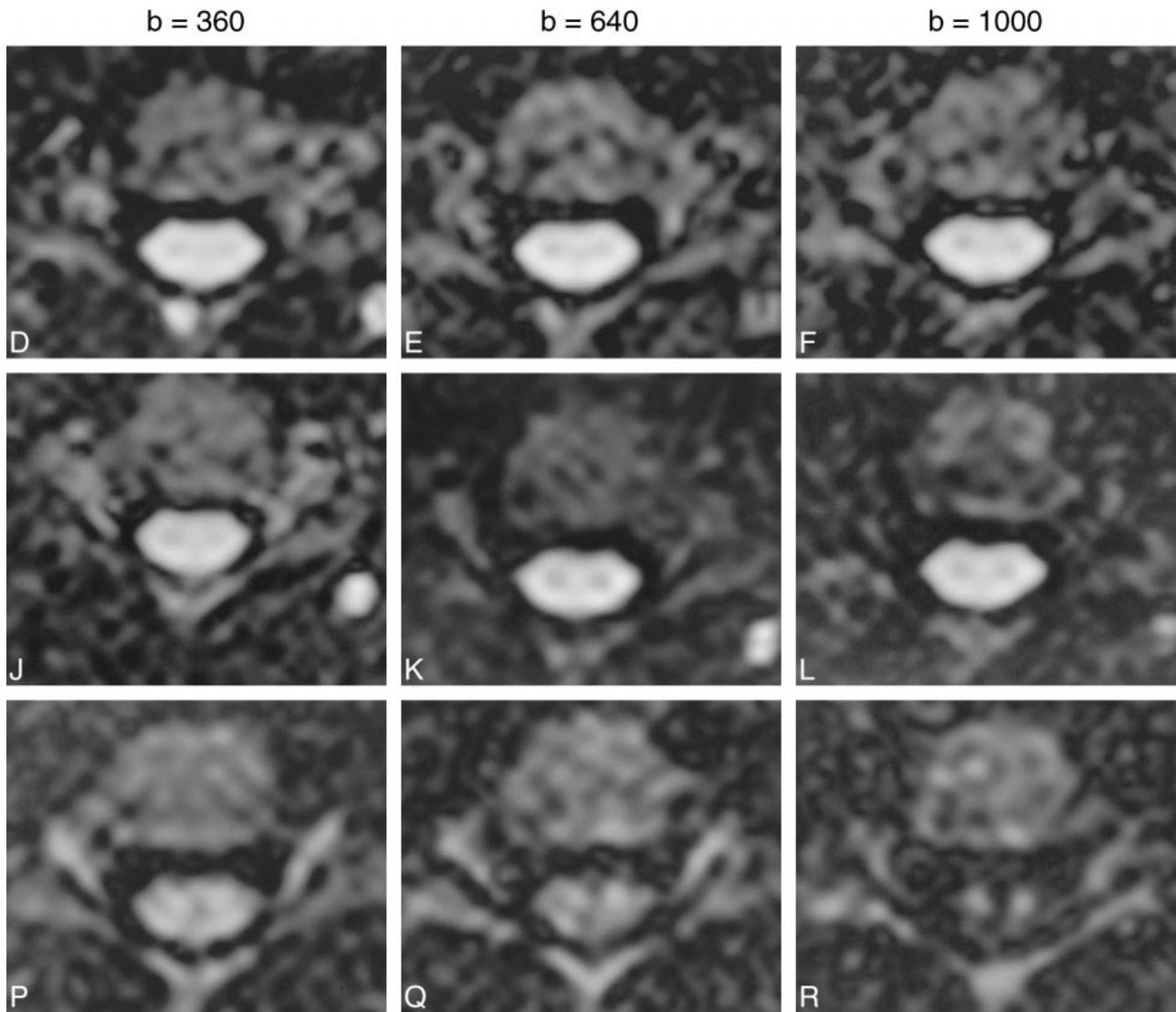


FIG 2. Axial diffusion-weighted images (2 R-R/106/4 [TR/TE/excitations]) showing the appearance of the cervical spinal cord with the diffusion-probing gradients in the three cardinal axes, with increasing  $b$  values from left to right. R-L, A-P, and C-C indicate the direction of the diffusion gradients. The R-L and A-P directions are perpendicular to the white matter tracts. The C-C direction is parallel to →

cord white matter (23, 28, 29). This may be due to the fact that our measurements were made *in vivo*, whereas the animal studies were performed on excised spinal cords, either fresh or fixed. In addition to being imaged at a lower temperature, which would lower the measured ADC values, the excised spinal cords would lack both microscopic (capillary) blood flow, which is believed to contribute to the ADC (7, 16), and axoplasmic flow, which has also been proposed to contribute to the diffusional anisotropy observed within axons (32). It is conceivable that changes in the viscoelastic properties of *ex vivo* and *in vivo* samples can affect diffusion measurements. Also, *ex vivo* spinal cords would almost certainly have ischemic changes, as have been well described in ischemic brain, resulting in restricted diffusion. All of these factors could theoretically result in a lower ADC value for *ex vivo* tissue relative to *in vivo* tissue, and explain the higher ADC values we calculated. Trudeau et al

(25), on the other hand, have reported similar anisotropy indices for the white matter in a freshly excised pig spinal cord model. Nakada and co-workers (31) have stated that diffusion within axons is virtually unrestricted in the longitudinal direction, which also supports our findings.

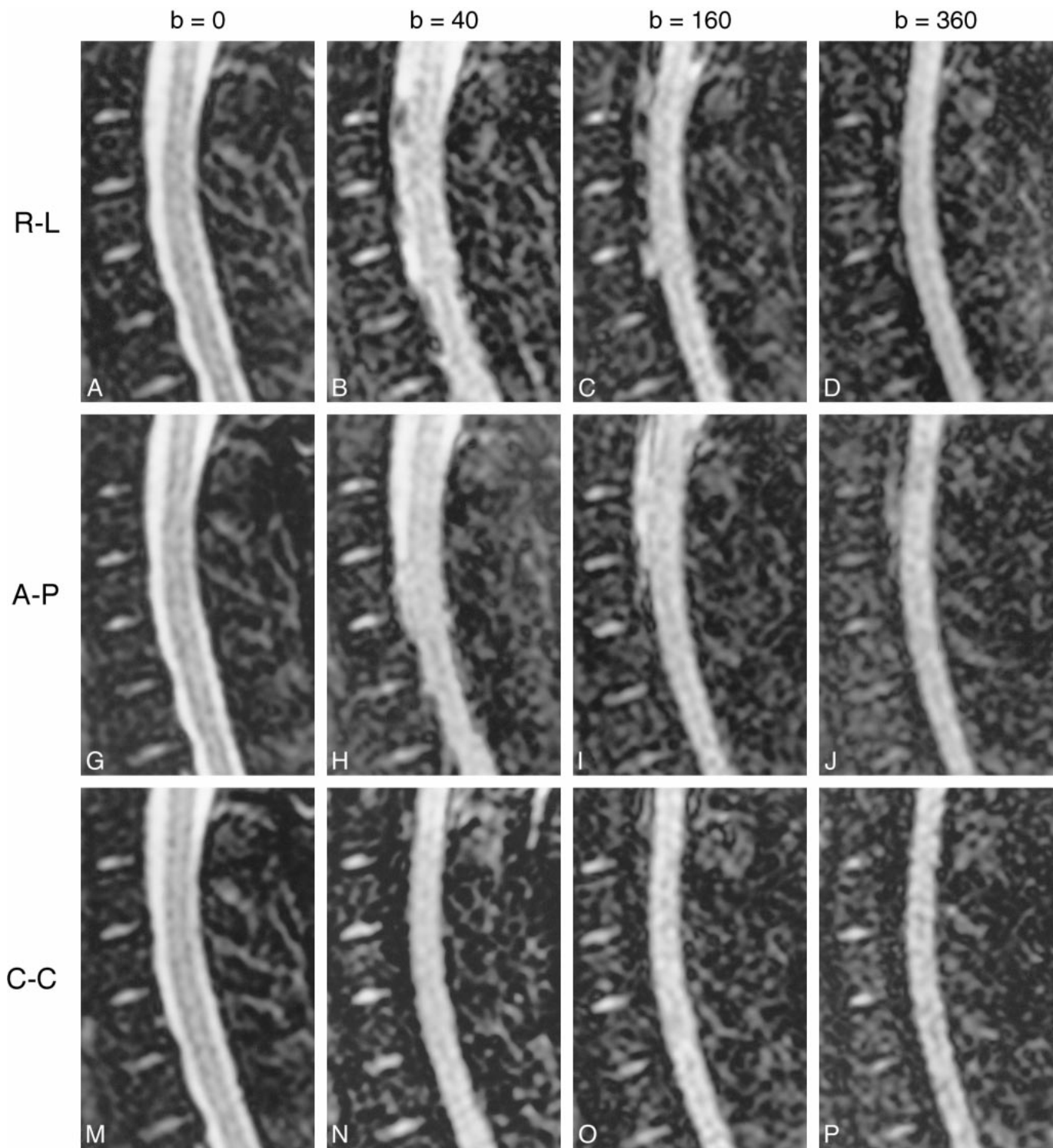
Given the highly ordered arrangement of axons in the spinal cord white matter tracts, it is not surprising that a statistically significant difference in ADCs between white matter and central gray matter was found, both in the axial and longitudinal diffusion directions. An unexpected finding was evidence of diffusional anisotropy within the central gray matter. Other investigators have reported anisotropy in excised animal spinal cord gray matter (23, 26, 28, 29, 36). There are at least three possible explanations for this observation. First, the relatively high ADC values measured in central gray matter with the diffusion-sensitizing gradients in the C-C direction may have been artifactually



(cont'd) the white matter tracts. Note the relatively greater signal attenuation with the diffusion gradients in the C-C direction, reflecting the underlying tissue anisotropy. Note also the reversal of the relative signal intensity of gray and white matter at the higher b values (640, 1000) in the C-C direction, due to the higher ADC of white matter along this axis.

elevated owing to partial volume averaging with adjacent white matter tracts. Although we cannot entirely exclude this possibility, it is less likely, because any effects of partial volume averaging would be expected to occur in all three directions. However, the measured ADC values for gray and white matter with the diffusion gradients in the A-P and R-L directions were within the expected range and relative magnitude, based on animal studies. Second, if there were cardiosynchronous pulsatile motion of the spinal cord in the longitudinal (C-C) direction, this could artificially elevate the measured ADCs of both the gray and white matter. However, our analysis of slices acquired at different cardiac phases did not indicate any changes in ADC associated with cardiac cycle. Nor did we observe a proportional elevation of the longitudinal ADC of the white matter beyond an expected range. In addition, any cardiosynchronous motion

would not necessarily occur in only one dimension, yet the measured ADC values in the axial plane were not similarly elevated. Also, the use of PPU triggering would tend to minimize any effects of periodic motion related to the cardiac cycle. The third possibility is that the monoexponential signal decay assumed in our studies does not adequately describe the diffusion occurring in the spinal cord tissue. It is known that conventional diffusion imaging experiments in the human brain (with  $b \sim 1000$  s/mm<sup>2</sup>) measure the average rate of diffusion without distinguishing the diffusion occurring in the extracellular (fast regime) and intracellular (slow regime) spaces. Recently, Bossart et al (36, 37), using very high magnetic field (14 T) strengths and large b values ( $b = 10,000$  s/mm<sup>2</sup>), characterized the fast and slow diffusion regimes in excised rat spinal cord specimens. Their results show that, in the slow diffusion regime, the gray matter dif-

Fig. 3  $\uparrow \rightarrow$ 

fusion is less restricted along the length of the cord than the white matter, while the converse is true in the fast diffusion regime. Although our experiments were not designed to resolve the fast and the slow diffusion regimes, these results confirm that diffusional anisotropy can exist in the gray matter. In light of these considerations, we believe that our observations are accurate, consistent with prior an-

imal studies, and these findings indicate the presence of diffusional anisotropy within human spinal cord gray matter as well as white matter. Clearly, the spatial resolution that we were able to obtain in the axial plane is a limitation of our study. Experiments with much higher spatial resolution and diffusion weighting are needed to understand the source of this observed apparent diffusional an-

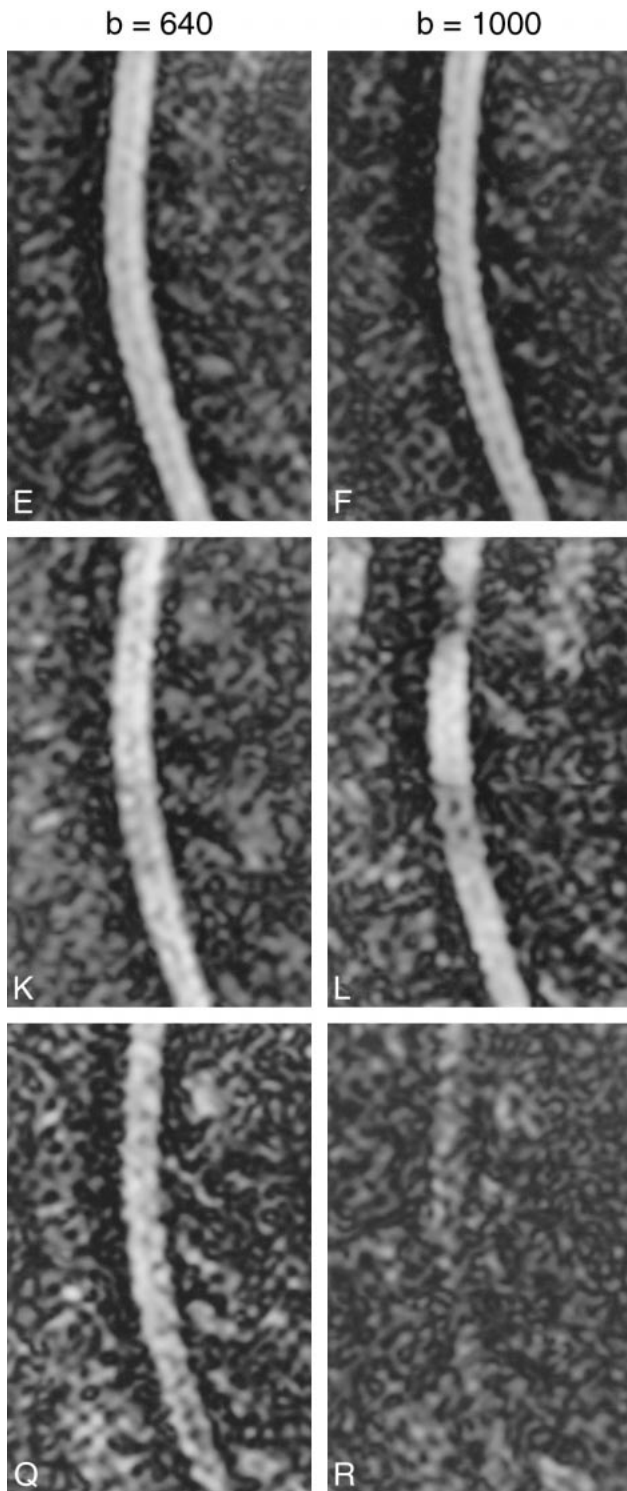


FIG 3. Sagittal diffusion-weighted images (2 R-R/106/4) showing the appearance of the cervical spinal cord with the diffusion-probing gradients in the three cardinal axes, with increasing  $b$  values from left to right. The R-L and A-P directions are perpendicular to the white matter tracts. The C-C direction is parallel to the white matter tracts. Again, there is relatively greater signal attenuation with the diffusion gradients in the C-C direction. Note the sensitivity of the diffusion-weighted sequence to pulsation at the highest  $b$  value in the A-P diffusion direction, resulting in artifact in the phase-encoding direction.

isotropy in gray matter in human spinal cord in vivo further.

### Conclusion

Small field-of-view diffusion-weighted images of the human spinal cord can be acquired in vivo on currently available MR imaging systems with reasonable scan times. The calculated longitudinal

ADC values observed were higher than previously published values for ex vivo animal spinal cord. Water mobility within the white matter of the human cervical spinal cord was found to be highly anisotropic. Evidence for in vivo diffusional anisotropy within human spinal cord gray matter, as suggested in animal studies, was also found, but was much lower than in white matter. This will require additional studies for confirmation and fur-

ther characterization. This technique provides unique tissue contrast and, if technical difficulties can be overcome, may prove useful for evaluation of a variety of pathologic conditions of the spinal cord.

## References

1. Le Bihan D, Turner R, Douek P, Patronas N. **Diffusion MR imaging: Clinical applications.** *AJR Am J Roentgenol* 1992;159:591-599
2. Chien D, Kwong KK, Gress DR, Buonanno FS, Buxton RB, Rosen BR. **MR diffusion imaging of cerebral infarction in humans.** *AJNR Am J Neuroradiol* 1992;13:1097-1102
3. Warach S, Chien D, Li W, Ronthal M, Edelman RR. **Fast magnetic resonance diffusion-weighted imaging of acute human stroke.** *Neurology* 1992;42:1717-1723
4. Larsson HBW, Thomsen C, Fredericksen J, Stubgaard M, Henriksen O. **In vivo magnetic resonance diffusion measurement in the brain of patients with multiple sclerosis.** *Magn Reson Imaging* 1992;10:7-12
5. Grossman RI, McGowan JC. **Perspectives on multiple sclerosis.** *AJNR Am J Neuroradiol* 1998;19:1251-1265
6. Liu AY, Maldjian JA, Bagley LJ, Sinson GP, Grossman RI. **Traumatic brain injury: diffusion-weighted MR imaging findings.** *AJNR Am J Neuroradiol* 1999;20:1636-1641
7. Le Bihan D, Breton E, Lallemand D, Grenier P, Cabanis EA, Laval-Jeantet M. **MR imaging of intravoxel incoherent motions: application to diffusion and perfusion in neurologic disorders.** *Radiology* 1986;161:401-407
8. Chien D, Buxton RB, Kwong KK, Brady TJ, Rosen BR. **MR diffusion imaging of the human brain.** *J Comput Assist Tomogr* 1990;14:514-520
9. Hajnal JV, Doran M, Hall AS, et al. **MR imaging of anisotropically restricted diffusion of water in the nervous system: technical, anatomic, and pathologic considerations.** *J Comput Assist Tomogr* 1991;15:1-18
10. Kim YJ, Chang K-H, Song IC, et al. **Brain abscess and necrotic or cystic brain tumor: Discrimination with signal intensity on diffusion-weighted MR imaging.** *AJR Am J Roentgenol* 1998;171:1487-1490
11. Tsuchiya K, Katase S, Yoshino A, Hachiya J. **Diffusion-weighted MR imaging of encephalitis.** *AJR Am J Roentgenol* 1999;173:1097-1099
12. Schaefer PW, Buonanno FS, Gonzalez RG, Schwamm LH. **Diffusion-weighted imaging discriminates between cytotoxic and vasogenic edema in a patient with eclampsia.** *Stroke* 1997;28:1082-1085
13. Schwartz RB, Mulkern RV, Gudbjartsson H, Jolesz F. **Diffusion-weighted MR imaging in hypertensive encephalopathy: Clues to pathogenesis.** *AJNR Am J Neuroradiol* 1998;19:859-862
14. Coley SC, Porter DA, Calamante F, Chong WK, Connelly A. **Quantitative MR diffusion mapping and cyclosporine-induced neurotoxicity.** *AJNR Am J Neuroradiol* 1999;20:1507-1510
15. Chenevert TL, Brunberg JA, Pipe JG. **Anisotropic diffusion in human white matter: demonstration with MR techniques in vivo.** *Radiology* 1990;177:401-405
16. Turner R, Le Bihan D, Maier J, Vavrek R, Hedges LK, Pekar J. **Echo-planar imaging of intravoxel incoherent motion.** *Radiology* 1990;177:407-414
17. Clark CA, Barker GJ, Tofts PS. **Magnetic resonance diffusion imaging of the human cervical spinal cord in vivo.** *Magn Reson Med* 1999;41:1269-1273
18. Ehman RL, Felmlee JP. **Adaptive technique for high-definition MR imaging of moving structures.** *Radiology* 1989;173:255-263
19. Anderson A, Gore J. **Analysis and correction of motion artifacts in diffusion-weighted imaging.** *Magn Reson Med* 1994;32:379-387
20. Ordidge RJ, Helpert JA, Qing ZX, Knight RA, Nagesh V. **Correction of motion artifacts in diffusion-weighted MR images using navigator echoes.** *Magn Reson Imaging* 1994;12:455-460
21. de Crespigny AJ, Marks MP, Enzmann DR, Moseley ME. **Navigated diffusion imaging of normal and ischemic human brain.** *Magn Reson Med* 1995;33:720-728
22. Butts K, de Crespigny AJ, Pauly JM, Moseley M. **Diffusion-weighted interleaved echo-planar imaging with a pair of orthogonal navigator echoes.** *Magn Reson Med* 1996;35:763-770
23. Pattany PM, Puckett WR, Klose KJ, et al. **High-resolution diffusion-weighted MR of fresh and fixed cat spinal cords: evaluation of diffusion coefficients and anisotropy.** *AJNR Am J Neuroradiol* 1997;18:1049-1056
24. Douek P, Turner R, Pekar J, Patronas N, Le Bihan D. **MR color mapping of myelin fiber orientation.** *J Comput Assist Tomogr* 1991;15:923-929
25. Trudeau JD, Dixon WT, Hawkins J. **The effect of inhomogeneous sample susceptibility on measured diffusion anisotropy using NMR imaging.** *J Magn Reson, Series B* 1995;108:22-30
26. Inglis BA, Yang L, Wirth ED, Plant D, Mareci TH. **Diffusion anisotropy in excised normal rat spinal cord measured by NMR microscopy.** *Magn Reson Imaging* 1997;15:441-450
27. Gulani V, Iwamoto GA, Jiang Hong, Shimony JS, Webb AG, Lauterbur PC. **A multiple echo pulse sequence for diffusion tensor imaging and its application in excised rat spinal cords.** *Magn Reson Med* 1997;38:868-873
28. Ford JC, Hackney DB, Alsop DC, et al. **MRI characterization of diffusion coefficients in a rat spinal cord injury model.** *Magn Reson Med* 1994;31:488-494
29. Schwartz ED, Yezierski RP, Pattany PM, Quencer RM, Weaver RG. **Diffusion-weighted MR imaging in a rat model of syringomyelia after excitotoxic spinal cord injury.** *AJNR Am J Neuroradiol* 1999;20:1422-1428
30. Moseley ME, Cohen Y, Kucharczyk J. **Diffusion-weighted MR imaging of anisotropic water diffusion in cat central nervous system.** *Radiology* 1990;176:439-445
31. Nakada T, Matsuzawa H, Kwee IL. **Magnetic resonance axonography of the rat spinal cord.** *NeuroReport* 1994;5:2053-2056
32. Matsuzawa H, Kwee IL, Nakada T. **Magnetic resonance axonography of the rat spinal cord: post-mortem effects.** *J Neurosurg* 1995;83:1023-1028
33. Dousset V, Franconi JM, Degreze P, Trillaud H, Pointillard V, Caille JM. **Anisotropic diffusion within the human spinal cord.** Proceedings of the 34th annual meeting of the American Society of Neuroradiology, Seattle, June 1996:257 (abstract)
34. Dousset V, Viaud B, Franconi JM, et al. **Diffusion imaging of the human spinal cord using steady-state free precession: application to cervical myelopathy.** Proceedings of the 35th annual meeting of the American Society of Neuroradiology, Toronto, May 1997:270 (abstract)
35. McKinnon GC. **Ultrafast interleaved gradient-echo-planar imaging on a standard scanner.** *Magn Reson Med* 1993;30:609-616
36. Bossart EL, Inglis BA, Buckley DL, Wirth ED, Mareci TH. **Multiple component diffusion tensor imaging in excised fixed CNS tissue.** Proceedings of the 7th annual meeting of the International Society for Magnetic Resonance in Medicine, Philadelphia, May 1999
37. Bossart EL, Inglis BA, Wirth ED, Mareci TH. **Multiexponential diffusion imaging of normal and 1-month post-injury rat spinal cords.** Proceedings of the 7th annual meeting of the International Society for Magnetic Resonance in Medicine, Philadelphia, May 1999